A study on photonic crystal slab waveguide with absolute photonic band gap

Materials Science

http://www.aimspress.com/journal/Materials

AIMS Materials Science, 5(1): 116–126.
DOI: 10.3934/matersci.2018.1.116
Received: 29 November 2017
Accepted: 24 January 2018
Published: 01 February 2018

Research article

A study on photonic crystal slab waveguide with absolute photonic band gap

Katsumasa Satoh and Yasuhide Tsuji*

Division of Information and Electronic Engineering, Muroran Institute of Technology, 27-1 Mizumoto-cho, Muroran, Hokkaido, 050-8585, JAPAN

* **Correspondence:** Email: y-tsuji@mmm.muroran-it.ac.jp; Tel: +81-143-46-5508; Fax: +81-143-46-5501.

Abstract: Most of the conventional photonic crystal (PhC) slab waveguides have a photonic band gap (PBG) only for one polarization state of two orthogonal polarization states. In this paper, we study on an absolute PBG that can realize PBG for both polarizations in the same frequency range and demonstrate that an absolute PBG can be realized in PhC structures proposed here. In the numerical analysis and design of PhC structures, we employ the two-dimensional finite element method (FEM) based on the effective index method (EIM). First, we propose two-types of PhC structures with an absolute PBG and show that a steering type PhC is superior to an air-ring type PhC to obtain a wideband absolute PBG. It is also shown that the optimized steering type PhC has the absolute PBG whose bandwidth of 164 nm at the center wavelength of 1.55 μm. Furthermore, we design PhC waveguides based on the obtained PhC structure having an absolute PBG in order to obtain guided modes for both polarization states within the same wavelength range. The transmission properties of the designed PhC waveguides are also investigated and 60 degree bends which are required in compact photonic circuits are designed. From these results, the possibility to realize compact polarization multiplexing photonic devices is shown.

Keywords: photonic crystal; absolute photonic band gap; photonic crystal waveguide; finite element method; effective index method

1. Introduction

With the recent development of optical communication systems, in order to realize high-speed and large-capacity photonic network, compact and high-performance optical waveguide devices have been intensively developed. Under these circumstances, several kinds of photonic crystals (PhCs) have been proposed as an artificial material and the photonic devices based on PhCs have attracted a lot of attentions [1–26]. PhCs are periodic nanoscale structures made of two or more kinds of dielectric

materials and some of them prohibit light propagation with specific frequency into them. This frequency band is referred to as photonic band gap (PBG) and is utilized to realize ultra-compact photonic devices since radiation loss at sharp bends is able to be suppressed. In view of actual fabrication, two-dimensional slab type PhCs are most widely discussed. In slab type PhCs, the PBG usually exists only for one polarization state of two orthogonal polarization states. If an absolute PBG for both polarization states is realized, the applicability of PhCs is further extended. For that reason, several types of PhC structures to realize absolute PBGs have been reported [2–16] and photonic devices utilizing an absolute PBG have been also reported [17–22]. However, in some of the PhCs proposed so far, the absolute PBGs have been realized in the higher frequency above light line. Therefore, in the actual application of those PhCs, the out-of-plane radiation loss may occur at waveguide discontinuities. Moreover, the most PhCs related to the absolute PBG has been studied in two-dimensional model. Although some PhCs with two- or three-dimensional structures have absolute PBGs below light line [11–16], these absolute PBGs do not exist between first and second photonic bands. In addition, these PhCs utilize anisotropic dielectric materials or three kinds of materials with higher refractive index to realize PhC slab with finite slab thickness. Considering to realize PhC devices on SOI platform, Si-based PhC seems to be preferable. In Ref. [9], it is demonstrated that the proposed Si-based honeycomb PhCs with finite slab thickness is able to realize an absolute PBG between first and second photonic bands. However, in this report, the approximated two-dimensional analysis is carried out and, in the actual three-dimensional model, the absolute PBG does not exist.

In this study, we propose novel Si-based PhCs with an absolute PBG and the structural parameters are optimized to expand a bandwidth of the absolute PBG. Through the numerical investigation in approximated two-dimensional model, it is shown that the optimized steering type PhC has the absolute PBG with a bandwidth of 164 nm at the center wavelength of 1.55 μm. Moreover, utilizing the designed PhC, we investigate the possibility of a compact photonic circuit which supports both polarization states. Finally, we analyze the dispersion property of the actual three-dimensional model of the proposed PhC and confirm the existence of an absolute PBG.

2. PhC with absolute PBG

In this discussion, the slab type PhCs consist of Silicon (Si) sandwiched by silica (SiO_2) is assumed and the slab thickness is set to be 240 nm. The refractive indices of Si, SiO_2, and air are assumed to be $n_{Si} = 3.4$, $n_{SiO_2} = 1.45$, and $n_{air} = 1$, respectively. For simplicity, by utilizing the effective index method (EIM) [27], the approximated two-dimensional models are discussed by using the finite element method (FEM) [28, 29] developed in our group and the effective indices are, respectively, assumed to be 2.83 and 2.16 for TE and TM wave analysis.

2.1. Dispersion property of air-ring type PhC

First, we consider an air-ring type PhC [22] shown in Figure 1a and discuss optimal parameters to realize absolute PBG. This PhC is considered as a compound PhC of air hole type and rod type PhCs. It becomes a conventional air hole PhC when the rod radius $r_1 = 0$. On the other hand, it becomes a rod type PhC when the air hole radius $r_2 = a/\sqrt{3}$. In general, air hole type PhCs have PBG for TE wave and rod type PhCs have PBG for TM wave. Thus, there seems to be a possibility to realize an

absolute PBG by the optimal selection of the parameters. Figure 1b shows the dependence of the PBG band on r_1 when r_2 is set to be $0.48a$. From this figure, we can see that the overlap of the PBGs for TE and TM waves is maximized at $r_1 = 0.29a$. Figure 1c shows the dispersion properties of the air-ring type PhC with $r_1 = 0.29a$ and $r_2 = 0.48a$. We can see that the absolute PBG exist in the normalized frequency range a/λ of $0.362 \sim 0.371$, in other words the mid-gap ratio $(\Delta\omega/\omega_0)$ is 2.46% where $\Delta\omega$ and ω_0 are, respectively, the bandwidth and central the frequency of the absolute PBG. Although the PBG is realized below the light line, the PBG band is not enough wide compared with PhCs made of anisotropic dielectrics [13–16].

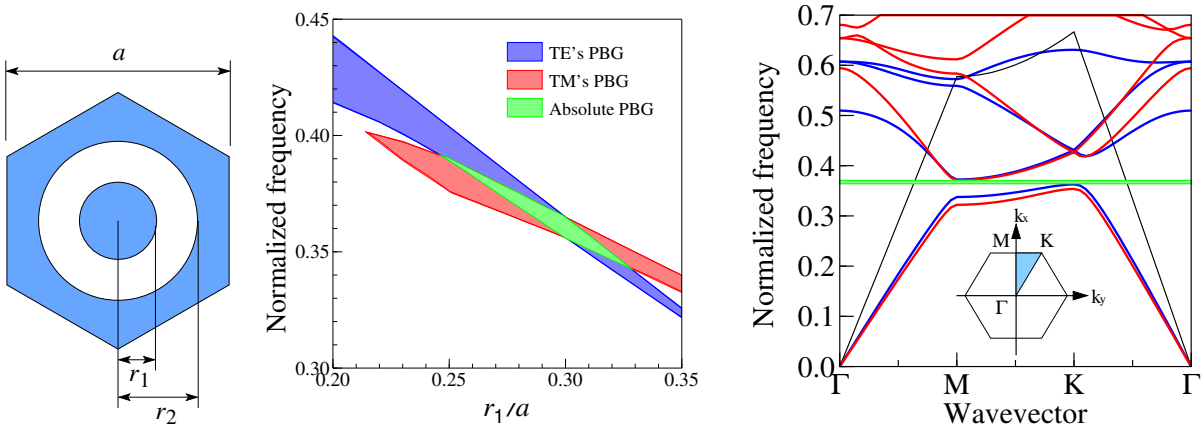

Figure 1. Air-ring type PhC. (a) Unit cell, (b) Dependence of the PBG band on r_1 when r_2, (c) Dispersion properties when $r_1 = 0.29a$ and $r_2 = 0.48a$.

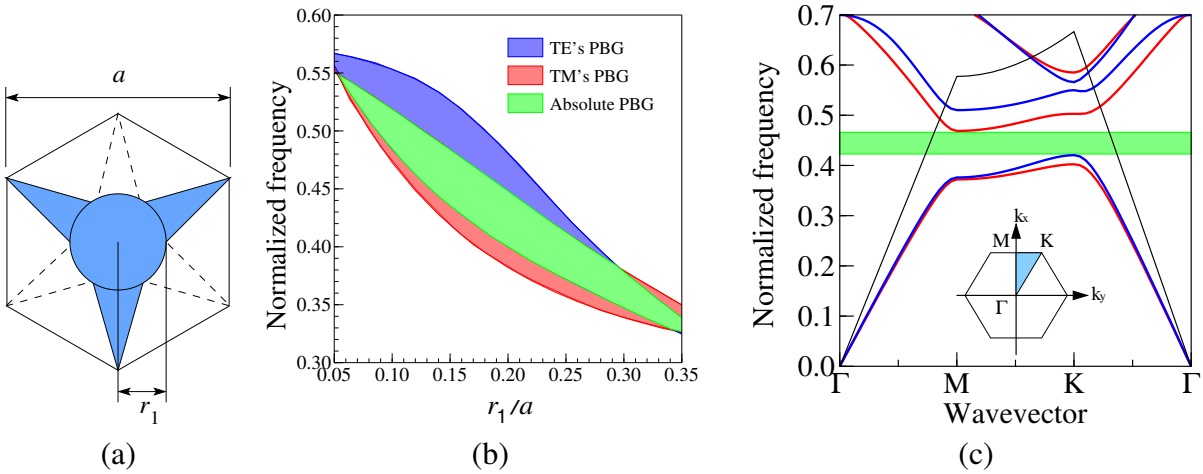

Figure 2. Steering type PhC. (a) Unit cell of steering type PhC, (b) Dependence of the PBG band on r_1, (c) Dispersion properties when $r_1 = 0.17a$.

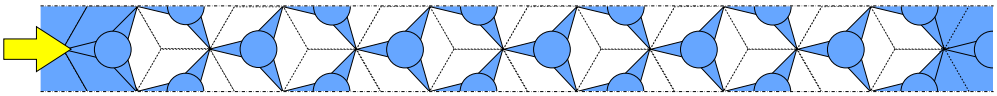

(a)

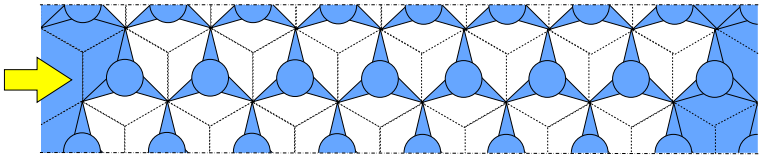

(b)

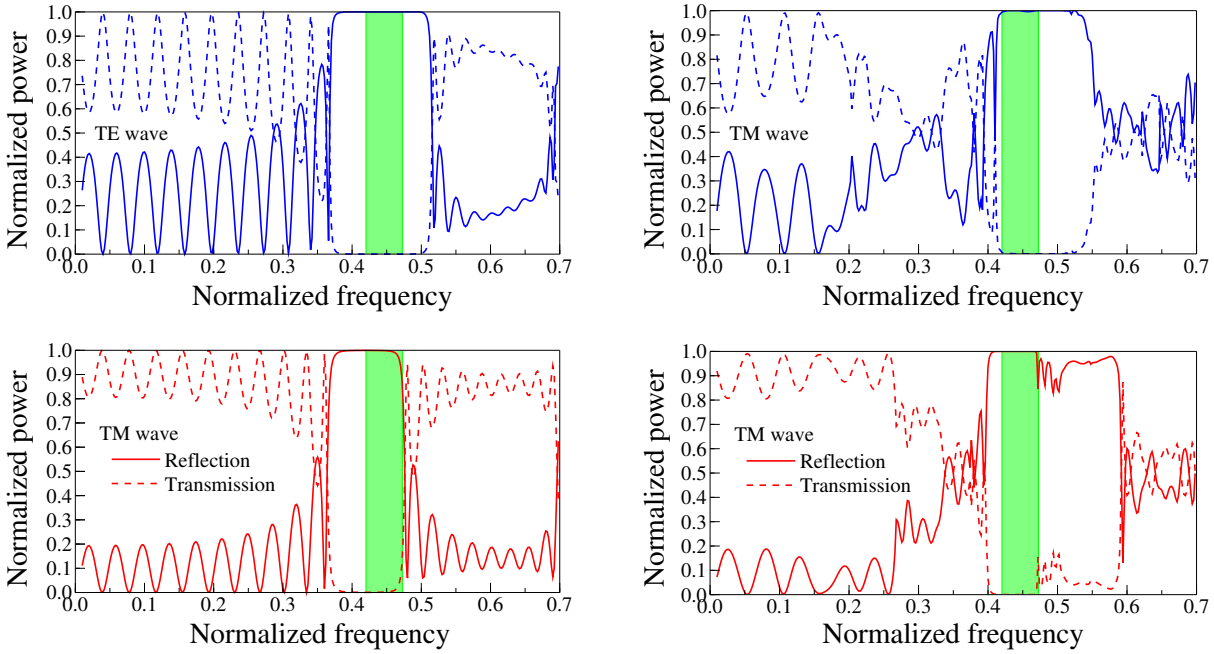

(c) (d)

Figure 3. Transmission and reflection properties of the steering type PhC with $r_1 = 0.29a$. (a) Computational model of Γ-K incidence case, (b) Computational model of Γ-M incidence case, (c) Transmission and reflection properties of Γ-K incidence case, (d) Transmission and reflection properties of Γ-M incidence case.

2.2. *Dispersion property of steering type PhC*

Next, in order to improve the bandwidth of an absolute PBG, we consider the PhC as shown in Figure 2a. We refer this type of PhC to as a steering type PhC. The steering type PhC is considered

to be a structure in which the position of the rod of the air-ring type PhC is shifted by $a/\sqrt{3}$ along y direction. Figure 2b shows the dependence of the PBG band on r_1. From this figure, we can see that the overlap of the PBGs for TE and TM waves is maximized at $r_1 = 0.17a$. Figure 2c shows the dispersion properties of the steering type PhC with $r_1 = 0.17a$. We can see that the absolute PBG exist in the normalized frequency range a/λ of $0.421 \sim 0.468$, in other words the mid-gap ratio is 10.57%. This result corresponds the wavelength bandwidth of 164 nm at the center wavelength of 1.55 μm. This PBG exist below light line and its bandwidth is greatly expanded compared with that of air-ring type PhC.

In order to confirm the existence of absolute PBG, we calculate the transmission property of this PhC with finite periods when plane waves are incident along Γ-K and Γ-M directions, respectively. The actual computational model shown in Figures 3a and b are considered. Figure 3c shows their transmission and reflection properties for Γ-K direction incidence case and Figure 3d shows them for Γ-M direction incidence case. We can see that the transmission and reflection spectra are totally complementary since material absorption losses are ignored in this calculation.

3. PhC waveguide based on steering type PhC

In the previous section, we discussed the air-ring and the steering type PhCs. Next, we discuss PhC waveguides based on PhC with absolute PBG. In this section, we consider only the steering type PhC whose PBG band is wider than that of air-ring type PhC. In the following discussion, r_1 is assumed to be $0.17a$.

Here, we consider two types of PhC waveguides shown in Figure 4. The PhC waveguide in Figure 4a is designed by filling the unit cells by Si. The dispersion properties of this PhC waveguide are shown in Figure 5. From these results, it can be seen that the single mode operation is realized for TM mode. However, the higher order mode of TE mode is observed. Figure 6 shows the propagating fields in the straight PhC at a normalized frequency of $a/\lambda = 0.44$. In this simulation, the PhC-based perfectly matched layer (PML) whose validity is confirmed in Ref. [30] is utilized as absorbing boundary conditions at the input and output end. We can see that, for both polarizations, the light is strongly confined in the core region owing to the absolute PBG. Next, we consider the 60 degree bend of this PhC waveguide. Figure 7 shows the structure of 60 degree bend and the propagating field through the bend. For TE mode, the excitation of the higher order mode is observed since this PhC waveguide is a multimode waveguide for TE mode. On the other hand, for TM mode, the higher order mode is not observed owing to the single mode operation although transmittance is fairly low. Thus, in order to improve the transmission property through waveguide bend, we modify the bending structure. Figure 8 shows the improved bend structure and the propagating fields. We can see that, for both modes, the transmission properties are greatly improved. However, for TE mode, higher order mode is still observed in the reflected wave.

Next, we consider the PhC waveguide shown in Figure 4b. Here, w is set to be $w = 0.58a$. Figure 9 shows the dispersion property of this waveguide. In this PhC waveguide, the single mode operation bands exist for both TE and TM modes although these bands do not overlap. Though polarization independent operation is not achieved in this PhC waveguide, polarization dependent devices, such as polarization splitter, is able to be designed using this PhC waveguide [18, 19]. Figure 10 shows the propagating fields in the straight PhC at a normalized frequency of $a/\lambda = 0.43$. We can see that, for

both polarizations, the light is strongly confined in the core region owing to the absolute PBG. Figure 11 shows the structure of 60 degree bend and the propagating field through the bend. We can see that the transmission properties are greatly improved compared with those of the previous examples.

(a) (b)

Figure 4. PhC waveguide based on the steering type PhC. (a) Type 1, (b) Type2.

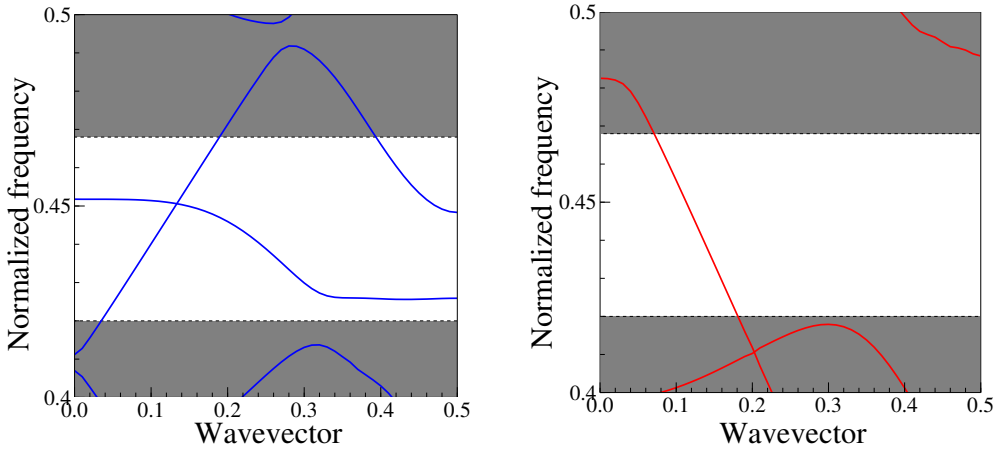

(a) (b)

Figure 5. Dispersion properties of Type 1 PhC waveguide. (a) TE mode, (b) TM mode.

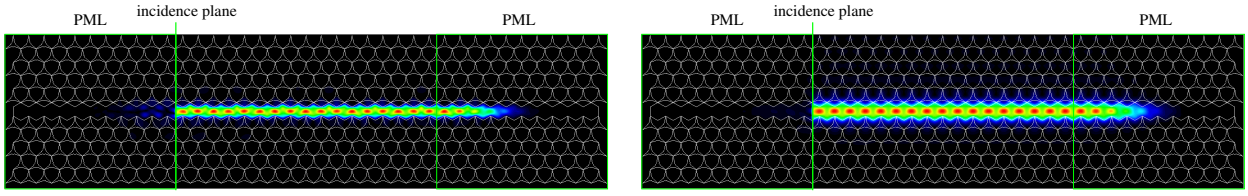

(a) (b)

Figure 6. Propagating field through Type 1 PhC waveguide. (a) TE mode, (b) TM mode.

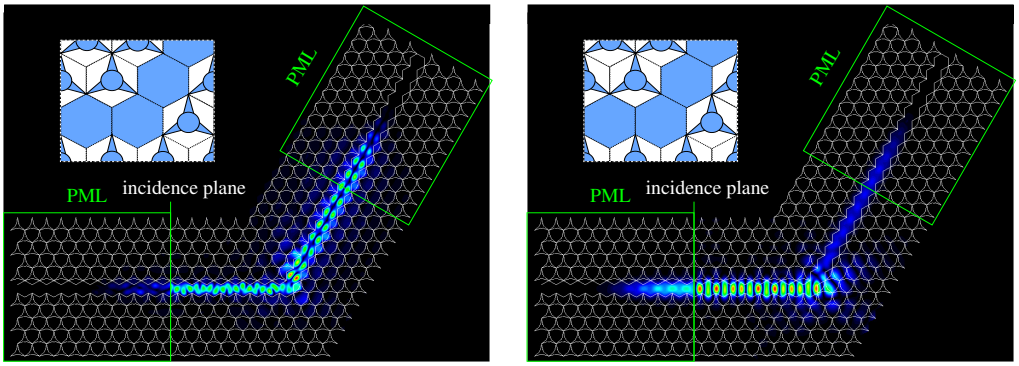

(a) (b)

Figure 7. Propagating field through 60 degree bend of Type 1 PhC waveguide. (a) TE mode, (b) TM mode.

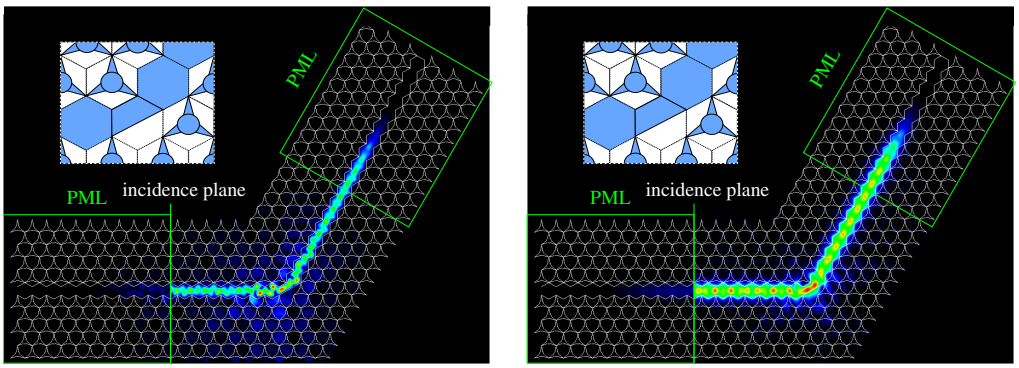

(a) (b)

Figure 8. Propagating field through improved 60 degree bend of Type 1 PhC waveguide. (a) TE mode, (b) TM mode.

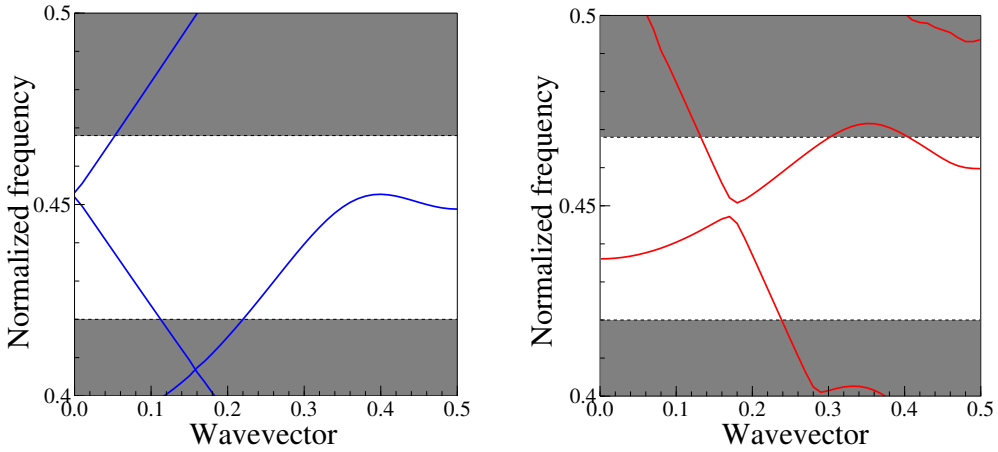

(a) (b)

Figure 9. Dispersion properties of Type 2 PhC waveguide. (a) TE mode, (b) TM mode.

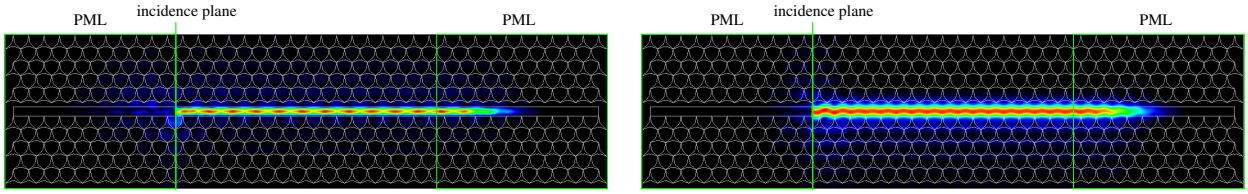

(a) (b)

Figure 10. Propagating field through Type 2 PhC waveguide. (a) TE mode, (b) TM mode.

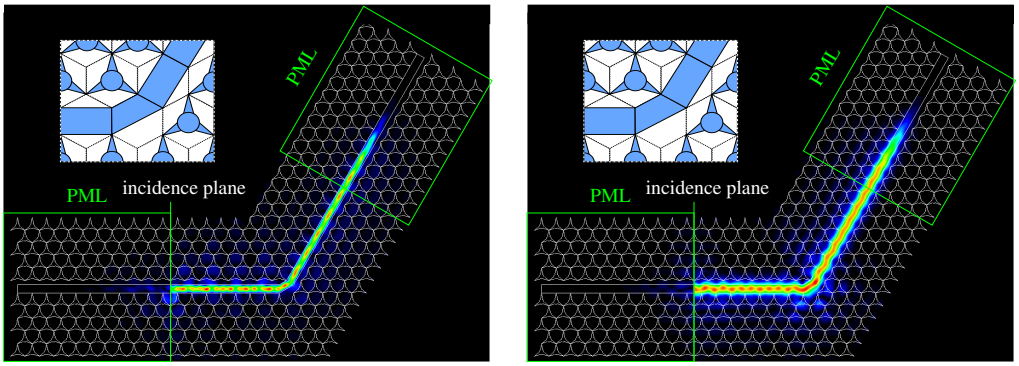

(a) (b)

Figure 11. Propagating field through 60 degree bend of Type 2 PhC waveguide. (a) TE mode, (b) TM mode.

4. Analysis of actual three-dimensional model

Finally, we analyze an actual three-dimensional structure of the proposed PhC by using three-dimensional full vector FEM [28] developed in our group. Although, in the previous two-dimensional model, the slab thickness is assumed to be $d = 240$ nm to use the effective index method, in this analysis, the slab thickness is defined by the normalized thickness and is assumed to be $d/a = 0.5$. Figures 12a and b show the unit cell and the periodic slab of the proposed PhC and Figure 12c shows its dispersion property. We can see that the absolute PBG exist in this PhC although the bandwidth is narrowed compared with the two-dimensional model. This is due to that the parameters are not optimized in the three-dimensional model. By optimizing the structural parameters in an actual three-dimensional model, the bandwidth of an absolute PBG is considered to be expanded.

5. Conclusions

We discussed novel photonic crystals which can realize absolute PBG. Furthermore, we designed the PhC waveguides based on the proposed PhCs and discussed the dispersion properties and the transmission properties through 60 degree bends. We are now studying the photonic devices utilizing absolute PBG, such as a polarization splitter, a polarization rotator, and an optical isolator. The design of photonic crystals with wider absolute PBG in an actual three-dimensional model is also now under consideration.

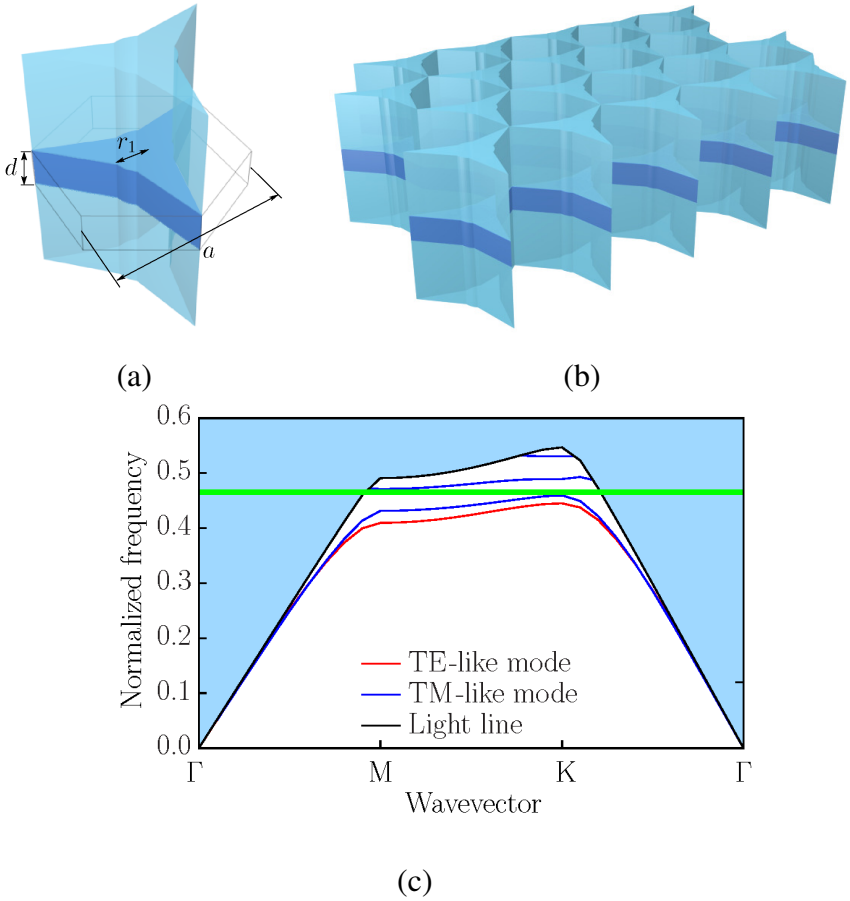

Figure 12. Actual three-dimensional steering type PhC slab. (a) unit cell, (b) periodic structure, (c) dispersion property.

Acknowledgments

This work was supported by JSPS KAKENHI Grant Number 15K06009.

Conflict of interest

The authors declare that there is no conflict of interest regarding the publication of this manuscript.

References

1. Joannopoulos JD, Villeneuve PR, Fan S (1997) Photonic crystals: pitting a new twist on light. *Nature* 386: 143–149.
2. Villeneuve PR, Piche M (1992) Photonic band gaps in two-dimensional square and hexagonal lattices. *Phys Rev B* 46: 4969–4972.
3. Anderson CM, Giapis KP (1996) Larger two-dimensional photonic band gaps. *Phys Rev Lett* 77: 2949–2951.

4. Kee CS, Kim JE, Park HY (1997) Absolute photonic bandgap in a two-dimensional square lattice of square dierectric rods in air. *Phys Rev E* 56: R6293.
5. Anderson CM, Giapis KP (1997) Symmetry reduction in group 4 mm photonic crystals. *Phys Rev B* 56: 7313–7320.
6. Qiu M, He S (1999) Large complete bandgap in two-dimensional photonic crystals with elliptic air holes. *Phys Rev B* 60: 10610–10612.
7. Shen L, He S, Xian S (2002) Large absolute band gaps in two-dimensional photonic crystals formed by large dielectric pixels. *Phys Rev B* 66: 165315.
8. Trifonov T, Marsal LF, Rodriguez A, et al. (2004) Effects of symmetry reduction in two-dimensional square and triangular lattices. *Phys Rev B* 69: 235112.
9. Wen F, David S, Checoury X, et al. (2008) Two-dimensional photonic crystals with large complete photonic band gaps in both TE and TM polarizations. *Opt Express* 16: 12278–12289.
10. Cerjan A, Fan S (2017) Complete photonic band gaps in supercell photonic crystals. *Phys Rev A* 96: 051802.
11. Kurt H, Citrin DS (2005) Annular photonic crystals. *Opt Express* 13: 10316–10326.
12. Kurt H, Hao R, Chen Y, et al. (2008) Design of annular photonic crystal slabs. *Opt Lett* 33: 1614–1616.
13. Shi P, Huang K, Kanng X, et al. (2010) Creation of large band gap with anisotropic annular photonic crystal slab structure. *Opt Express* 18: 5221–5228.
14. Razari B, Kalafi M (2006) Engineering absolute band gap in anisotropic hexagonal photonic crystals. *Opt Commun* 266: 159–163.
15. Razari B, Khalkhali FT, Bala AS, et al. (2009) Absolute band gap properties in two-dimensional photonic crystals composed of air rings in anisotropic tellurium background. *Opt Commun* 282: 2861–2869.
16. Khalkhali FT, Razari B, Kalafi M (2011) Enlargement of absolute photonic band gap in modified 2D anisotropic annular photonic crystals. *Opt Commun* 284: 3315–3322.
17. Erol AE, Sözüer HS (2015) High transmission through a 90° bend in a polarization-independent single-mode photonic crystal waveguide. *Opt Express* 23: 32690–32695.
18. Tsuji Y, Morita Y, Hirayama K (2006) Photonic crystal waveguide based on 2-D photonic crystal with absolute photonic band gap. *IEEE Photonic Tech L* 18: 2410–2412.
19. Morita Y, Tsuji Y, Hirayama K (2008) Proposal for a compact resonant-coupling-type polarization splitter based on photonic crystal waveguide with absolute photonic bandgap. *IEEE Photonic Tech L* 20: 93–95.
20. Wu H, Citrin DS, Jiang L, et al. (2015) Polarization-Independent Single-Mode Waveguiding With Honeycomb Photonic Crystals. *IEEE Photonic Tech L* 27: 840–843.
21. Rani P, Kara Y, Sinha RK (2016) Design and analysis of polarization independent all-optical logic gates in silicon-on-insulator photonic crystal. *Opt Commun* 374: 148–155.
22. S*äynä*tjoki A, Mulot M, Ahopelto J, et al. (2007) Dispersion engineering of photonic crystal waveguides with ring-shaped holes. *Opt Express* 15: 8323–8328.

23. Hou J, Citrin DS, Wu H, et al. (2011) Enhanced bandgap in annular photonic-crystal silicon-on-insulator asymmetric slabs. *Opt Lett* 36: 2263–2265.
24. Wang F, Cheng YZ, Wang X, et al. (2018) Effective modulation of the photonic band gap based on Ge/ZnS one-dimensional photonic crystal at the infrared band. *Opt Mater* 75: 373–378.
25. Wang X, Qi D, Wang F, et al. (2017) Design and fabrication of energy efficient film based on one-dimensional photonic band gap structures. *J Alloy Compd* 697: 1–4.
26. Qi D, Wang X, Cheng Y, et al. (2016) Design and characterization of one-dimensional photonic crystals based on ZnS/Ge for infrared-visible compatible stealth applications. *Opt Mater* 62: 52–56.
27. Okamoto K (2005) *Fundamentals of optical waveguides*, 2Eds, Academic Press.
28. Koshiba M (1992) *Optical waveguide theory by the finite element method*, Tokyo/Dordrecht: KTK Scientific Publishers/Kluwer Academic Publishers.
29. Tsuji Y, Koshiba M (2002) Finite element method using port truncation by perfectly matched layer boundary conditions for optical waveguide discontinuity problems. *J Lightwave Technol* 20: 463–468.
30. Koshiba M, Tsuji Y, Sasaki S (2001) High-performance absorbing boundary conditions for photonic crystal waveguide a simulations. *IEEE Microw Wirel Co* 11: 152–154.

AIMS Press